Supporting Information for

Photosensitizing Covalent Organic Frameworks for Activating Polyoxometalates toward Efficient Photocatalytic Sulfide Oxidation

Yanyan Guo [ab, 1], Jialing Chen [a, 1], Na Xu*[a], Ye Chen[b] Xiuli Wang *[a]

[a] *College of Chemistry, Bohai University, Professional Technology Innovation Center of Liaoning Province for Conversion Materials of Solar Cell, Jinzhou 121013, PR China*

[b] *State Key Laboratory of Advanced Fiber Materials, College of materials science and engineering, Donghua University, Shanghai, 201620, China*

Table of Contents

Experimental section

Materials and methods

1, 3, 5–triformylphloroglucinol (Tp), TG were purchased from Jilin Research and Extension Technology Company. Keggin–type $H_3PMo_{12}O_{40}$ (PMo_{12}), $H_3PW_{12}O_{40}$ (PW_{12}), $H_3SiW_{12}O_{40}$ (SiW_{12}), mesitylene, 1,4–dioxane were all purchased by Aladdin Reagents. Powder X–ray diffraction (PXRD) patterns were measured on a D/teX Ultra diffractometer with Cu Kα radiation (λ = 1.5418 Å). Diffraction intensity data were collected with 2θ values ranging from 3° to 50° at a scanning speed of 2°/min and a step size of 0.01°. FT-IR spectroscopy was performed on a Perkin Elmer spectrometer in the wavenumber range of 500–4000 cm^{-1}. Thermogravimetric analyses were conducted using a Hitachi TG/DTA7200 analyzer under N_2 flow with a heating rate of 10 °C/min from 25 to 800 °C. Scanning electron microscope (SEM) images and energy-dispersive spectroscopy (EDS) were acquired on a cold field-emission scanning electron microscope (S-4800). Transmission electron microscopy (TEM) was performed on a JEOL JEM-2100F operated at 200 kV, equipped with an EDS detector (X-MaxN 80T IE250). UV-Vis absorption spectra were collected on an SP 1901 UV-Vis spectrophotometer. X-ray photoelectron spectroscopy (XPS) was performed using a Thermo Scientific K-Alpha photoelectron spectrometer. Elemental analysis was conducted on a UNICUBE-Elementar analyzer.

Electrochemical Measurements

Electrochemical impedance spectroscopy (EIS), photoelectrochemical measurements, and Mott-Schottky plots were carried out on a CHI-760 workstation. The experimental conditions are as follows: (1) Reference electrode: Ag/AgCl; the potential was converted to the NHE scale via ENHE = EAg/AgCl + 0.197 V. (2) Working electrode: FTO conductive glass (1.0 cm^2). (3) Electrolyte: 0.1 M Na_2SO_4 (pH = 7.0).

Photocatalytic Reaction

The photocatalytic oxidation of sulfides was performed as follows: MPS (0.5 mmol), catalyst (0.7 mmol%), naphthalene (internal standard, 15 mg), solvent (3 mL), 25 °C (thermostated), 300 W Xe lamp. The photocatalytic activity of Keggin-type POM@TpTG composites (PW_{12}, PMo_{12}, SiW_{12}) for sulfide oxidation was evaluated under visible light (λ ≥ 425 nm) using 30% H_2O_2 as oxidant. After the reaction was completed, the solution was filtered through a filter membrane (pore size: 0.22 μm,

diameter: 13 mm). The reaction mixture was analyzed using a Shimadzu GC-7900 gas chromatograph equipped with a TM-5 Sil capillary column and a flame ionization detector (FID). The injection volume was 1 μL, and the column was maintained at 150 °C for 9 min. Naphthalene was used as the internal standard for quantitative analysis, and the product yield was calculated by the internal standard method.

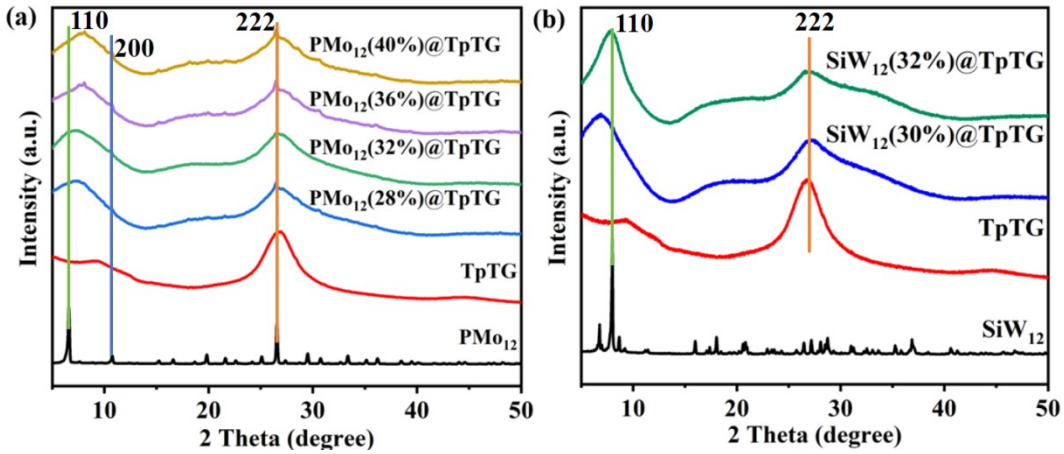

Fig. S1 (a) PXRD patterns of PMo_{12}, TpTG and PMo_{12}@TpTG; (b) PXRD patterns of SiW_{12}, TpTG and SiW_{12}@TpTG.

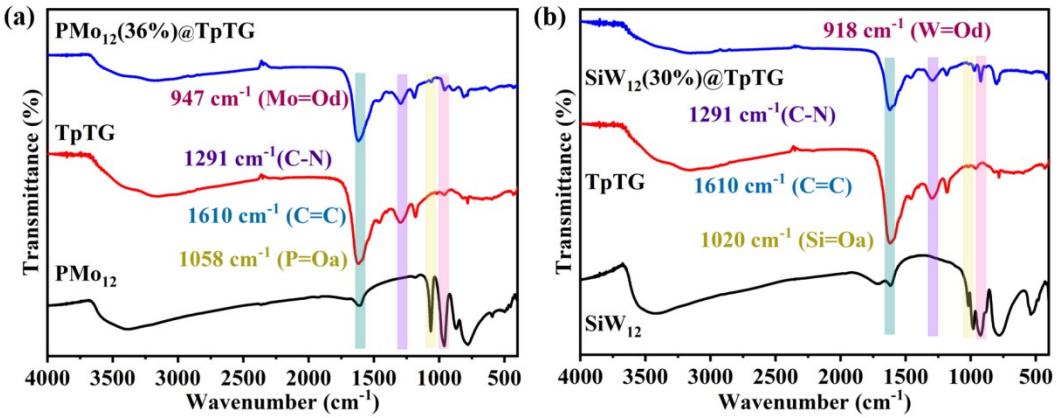

Fig. S2 (a) FT-IR spectra of TpTG, PMo_{12}@TpTG and PMo_{12}; (b) FT-IR spectra of SiW_{12}, TpTG and SiW_{12}@TpTG.

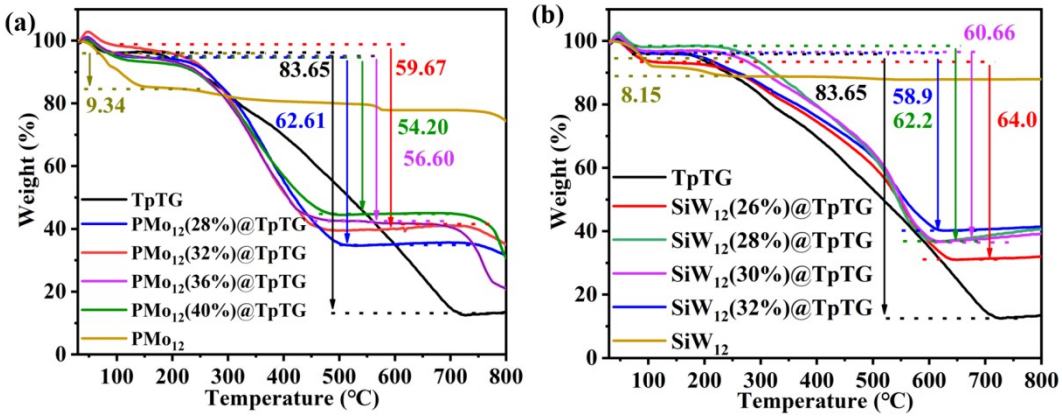

Fig. S3 (a) TGA of TpTG, PMo_{12}@TpTG and PMo_{12}; (b) TGA of TpTG, SiW_{12}@TpTG and SiW_{12}.

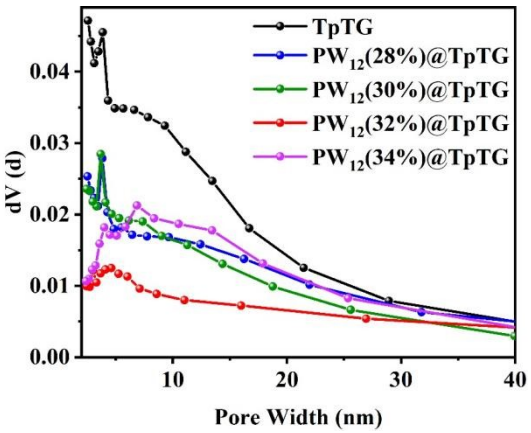

Fig. S4 Aperture diagram of TpTG, PW_{12}, PW_{12}(28%)@TpTG, PW_{12}(30%)@TpTG, PW_{12}(32%)@TpTG, and PW_{12}(34%)@TpTG.

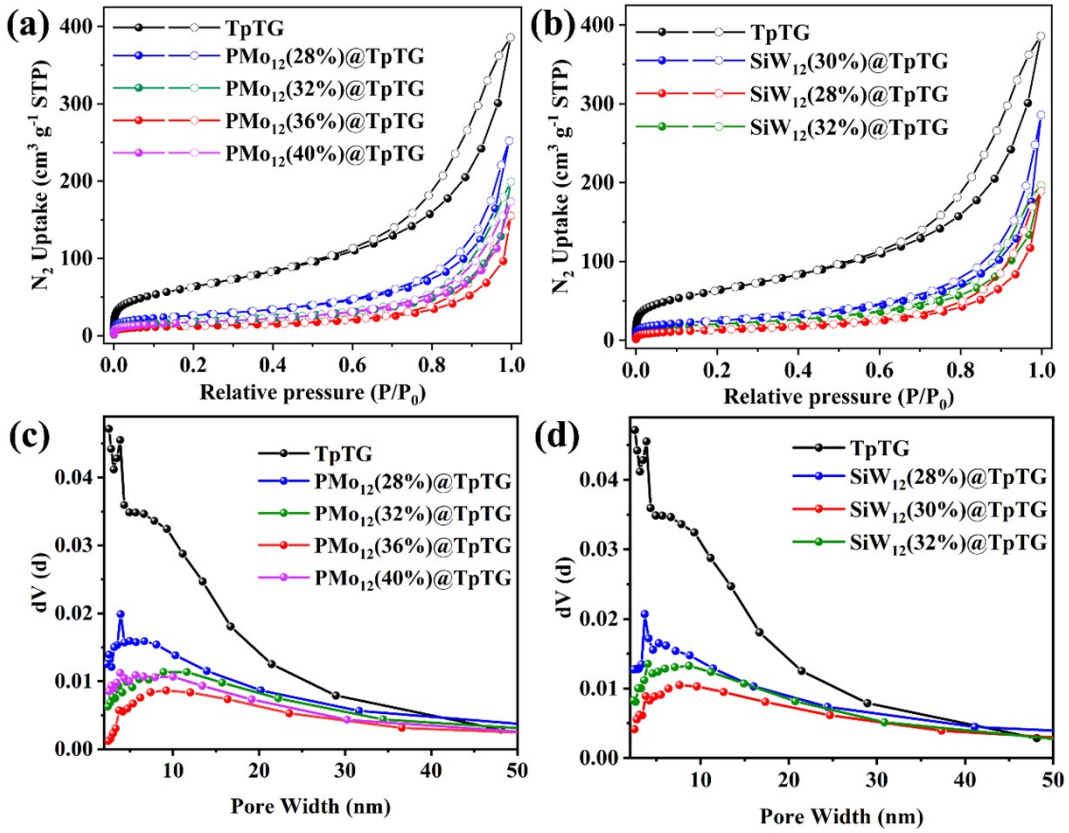

Fig. S5 (a) N_2 sorption isotherms of TpTG and different PMo_{12} added amounts of PMo_{12}@TpTG measured at 77 K; (b) N_2 sorption isotherms of TpTG and different SiW_{12} added amounts of SiW_{12}@TpTG measured at 77 K; (c)The pore size distribution of TpTG and PMo_{12}@TpTG; (d)The pore size distribution of TpTG and SiW_{12}@TpTG.

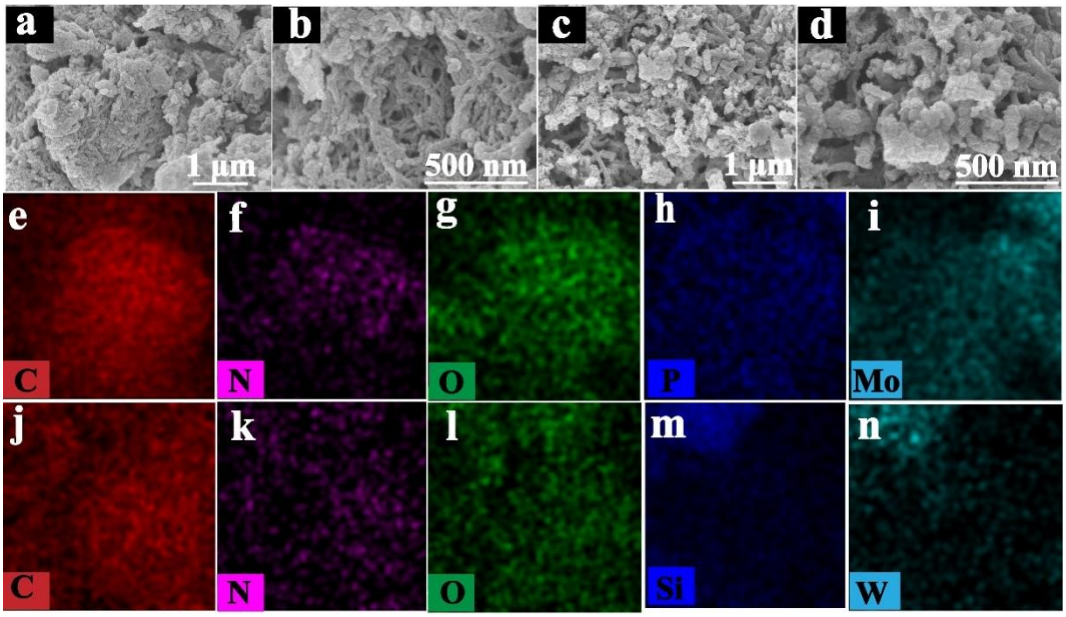

Fig. S6 (a–b) SEM image of PMo_{12}(36%)@TpTG; (c–d) SEM images of SiW_{12}(30%)@TpTG; (e–i) EDS images of PMo_{12}(36%)@TpTG; (j–n) EDS mapping images of SiW_{12}(30%)@TpTG.

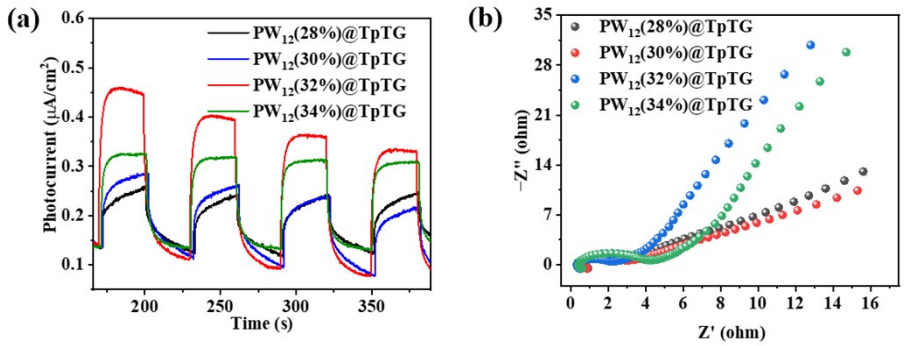

Fig. S7 (a) Transient photocurrent responses of PW_{12}(28%)@TpTG, PW_{12}(30%)@TpTG, PW_{12}(32%)@TpTG, and PW_{12}(34%)@TpTG; (b) EIS Nyquist plots of PW_{12}(28%)@TpTG, PW_{12}(30%)@TpTG, PW_{12}(32%)@TpTG, and PW_{12}(34%)@TpTG.

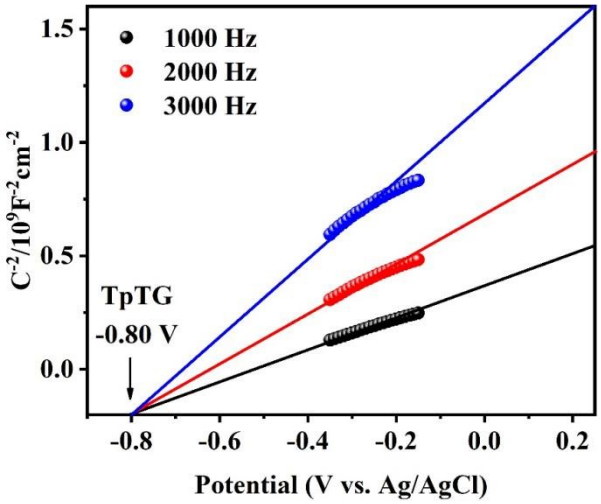

Fig. S8 M-S plots of TpTG.

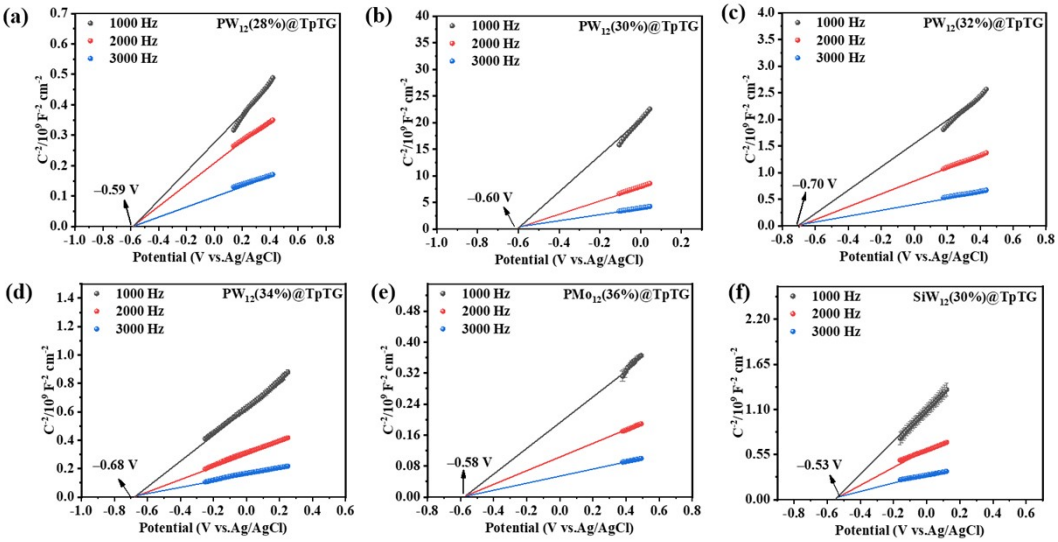

Fig. S9 M-S plots of (a) PW_{12}(28%)@TpTG, (b) PW_{12}(30%)@TpTG, (c) PW_{12}(32%)@TpTG, (d) PW_{12}(34%)@TpTG, (e) PMo_{12}(36%)@TpTG, and (f) SiW_{12}(30%)@TpTG.

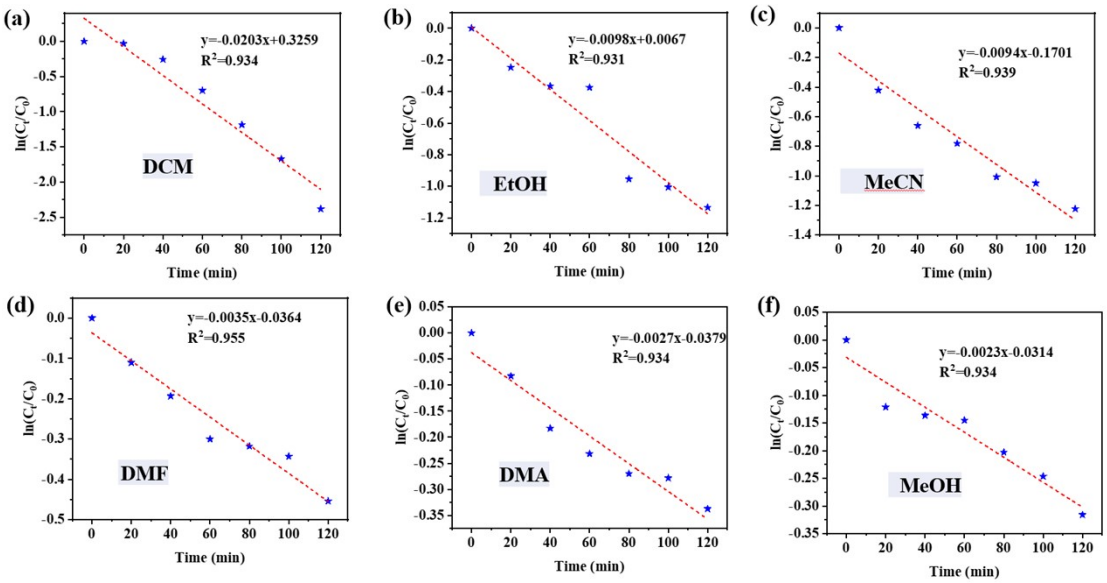

Fig. S10 Reaction kinetics of PW_{12}(34%)@TpTG under different solvent conditions.

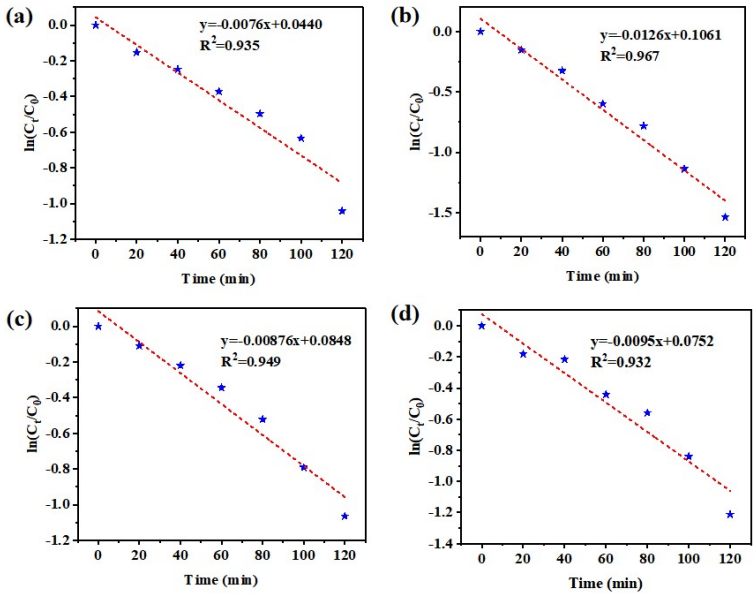

Fig. S11 Effect of H_2O_2 dosage on MPS oxidation: (a) 1.1 mmol, (b) 1.2 mmol, (c) 1.3 mmol, and (d) 1.5 mmol.

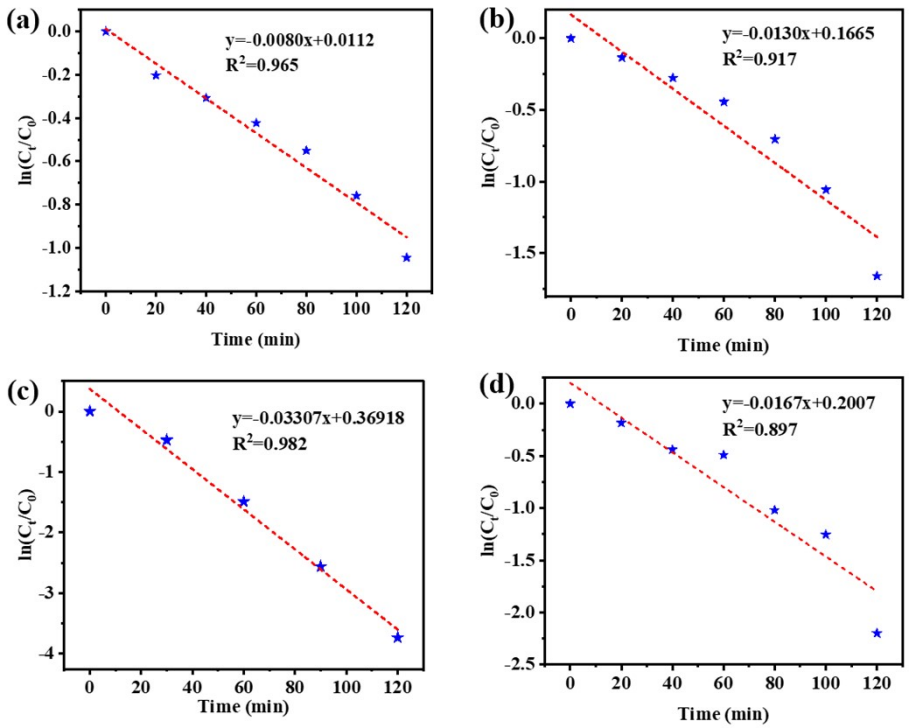

Fig. S12 Kinetic plots of MPS oxidation over PW_{12}@TpTG with different PW_{12} loadings: (a) 28%, (b) 30%, (c) 32%, and (d) 34%.

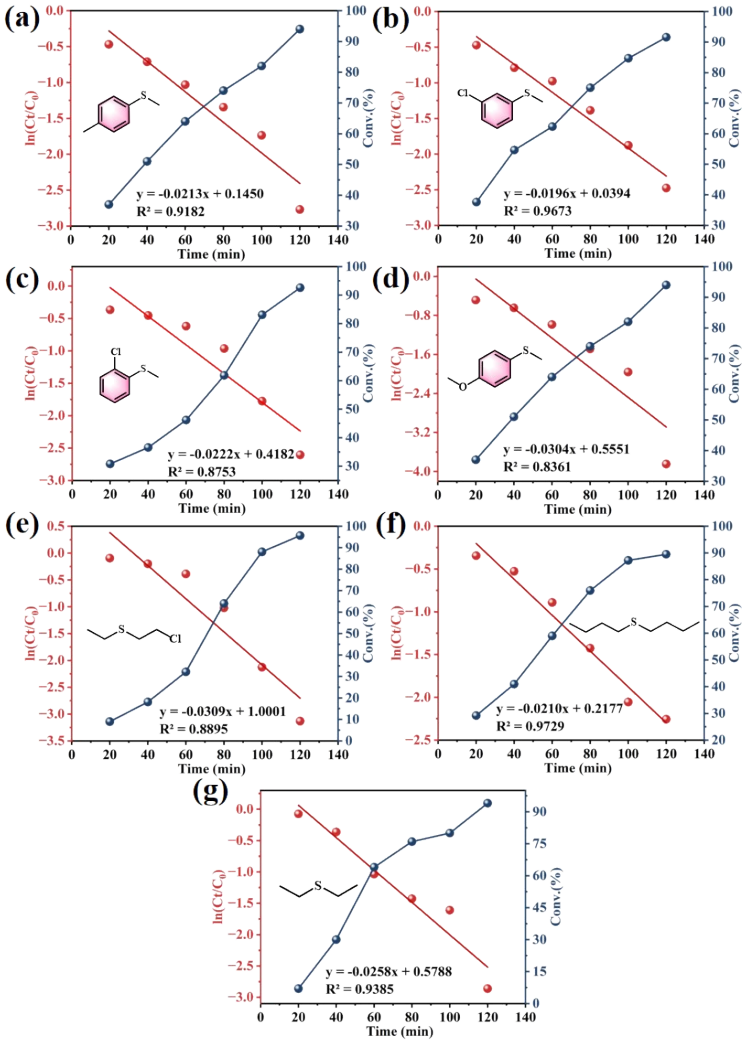

Fig. S13 Pseudo-first-order kinetic plots for the oxidation of (a) methyl phenyl sulfide, (b) 3-chloro methyl phenyl sulfide, (c) 2-chloro methyl phenyl sulfide, (d) methoxy methyl phenyl sulfide, (e) 2-chloroethyl sulfide, (f) diethyl sulfide, and (g) dipropyl sulfide.

Table S1 Physicochemical properties of POM@TpTG composites.

Composites	S_{BET} ($m^2 \cdot g^{-1}$)	Vtotal ($cc \cdot g^{-1}$)	Average pore size (nm)
TpTG	230.84	0.60	5.17
PW_{12}(28%)@TpTG	133.60	0.44	6.52
PW_{12}(30%)@TpTG	123.69	0.34	5.54
PW_{12}(32%)@TpTG	43.05	0.27	5.88
PW_{12}(34%)@TpTG	111.90	0.39	6.96
PMo_{12}(28%)@TpTG	92.70	0.39	8.42
PMo_{12}(32%)@TpTG	63.76	0.31	9.66

PMo_{12}(36%)@TpTG	42.85	0.24	11.2
PMo_{12}(40%)@TpTG	60.85	0.27	8.82
SiW_{12}(28%)@TpTG	88.67	0.44	9.98
SiW_{12}(30%)@TpTG	48.50	0.30	6.94
SiW_{12}(32%)@TpTG	73.40	0.30	8.28

Table S2 The photoelectric performance and catalytic rate of PW_{12}@TpTG.

Sample	Photocurrent density ($\mu A/cm^2$)	Rct (Ω)	k_{rec} (s^{-1})	Rate constant k (min^{-1})
PW_{12}(28%)@TpTG	2.0	1250	0.85	0.0080
PW_{12}(30%)@TpTG	3.0	1120	0.72	0.0130
PW_{12}(32%)@TpTG	4.5	620	0.48	0.0330
PW_{12}(34%)@TpTG	3.2	880	0.65	0.0167

Table S3 Solvent effect on the photocatalytic oxidation of MPS.

Solvent	Dielectric constant (ε)	Rate constant k (min^{-1})	Con. (%)	Sel. (%)
CHY	2.02	0.0331	99.0	99.6
DCM	8.93	0.0203	90.8	99.0
EtOH	24.3	0.0098	67.8	32.2
MeCN	37.5	0.0094	70.6	29.4
DMF	38.3	0.0035	36.5	63.5
DMA	37.8	0.0027	28.6	71.4
MeOH	32.7	0.0023	27.0	72.9

Table S4 The oxidation effect of POM@TpTG composites with different POMs loadings on photocatalytic MPS was studied. [a]

Entry	Catalyst	Conv. (%)	Sel.[b] (%)
1	PW_{12}(30%)@TpTG	93.7	99.5
2	PW_{12}(32%)@TpTG	99.0	99.6
3	PW_{12}(34%)@TpTG	98.2	99.5
4	PMo_{12}(28%)@TpTG	88.1	98.4
5	PMo_{12}(32%)@TpTG	92.3	99.1
6	PMo_{12}(36%)@TpTG	96.0	99.0
7	SiW_{12}(28%)@TpTG	40.7	77.1
8	SiW_{12}(30%)@TpTG	45.0	77.9
9	SiW_{12}(32%)@TpTG	41.3	65.9

[a] Reaction conditions: 0.5 mmol MPS, 0.7 mmol% PW_{12}(32%)@TpTG material, 1.3 mmol H_2O_2, 25 °C 300 W Xe lamp and reaction time 2.0 h; [b] the main product of is sulfone.

Table S5 The Comparison of the photocatalytic performance of PW_{12}@TpTG with state-of-the-art COF/MOF/POM-based photocatalysts for sulfide oxidation.

Catalyst	Substrate	Light source	Time	Conv. (%)	Sel. (%)	Ref.
PW_{12}@TpTG	MPS	300 W Xe lamp (λ ≥ 425 nm)	2 h	99.0	99.6	This work
TpBpy-COF	MPS	blue LED	6 h	99.9	99.9	[1]
P_2W_{18}-COF	MPS	10 W white LED	18 min	99	97	[2]
SiW_{12}-CTF	MPS	10 W 425 nm LED	2 h	97	99	[3]
PW_{12}-CTF	MPS	10 W 425 nm LED	2 h	89	99	[3]
PMo_{12}-CTF	MPS	10 W 425 nm LED	2 h	36	99	[3]
SiW_{12}-CTF-2	MPS	10 W 425 nm LED	2 h	81	99	[3]
PMo_{12}(46.1%)@ RT-COF-1	MPS	Ultrasound-assisted	2 h	49.5	16.6	[4]
HY-340	MPS	60 °C, 0.2 mL H_2O_2,	2 h	100	70	[5]

Table S6 The selective oxidation of CEES catalyzed by PW_{12}(32%)@TpTG was studied. [a]

Entry	Catalyst (mmol%)	H_2O_2 (mmol)	Conv. [b](%)	Sel. [c](%)
1	0.8	1.4	86.9	100
2	0.9	1.4	99.4	100
3	1.1	1.4	98.2	100
4	0.9	1.1	93.1	100
5	0.9	1.2	95.7	100
6	0.9	1.3	96.1	100
7	0.9	1.3	98.7	100
8	0.9	–	28.0	86.8
9	–	1.3	47.6	94.5
10	–	–	Trace	Trace

[a] Reaction conditions: 0.5 mmol CEES and 3 mL CYH, 25 °C 300 W Xe lamp and reaction time 1.5 h; [b] measured by GC; [c] selectivity of $CEESO_2$.

Table S7 ICP-OES analysis of tungsten (W) leaching from PW_{12}@TpTG catalyst after one catalytic cycle.

Sample	W(mg/L) [a]	W (mg/mL)
Reference material	–0.0208	0
After 1st cycle	0.0155	7.75×10^{-4}

After 2nd cycle	–0.0176	0
After 3st cycle	–0.0229	0
After 4st cycle	–0.0210	0
After 5st cycle	–0.0231	0

[a] Dilute 1 mL of sample to volume, test result of 50 mL

Table S8 PW_{12}(32%)@TpTG photocatalytic oxidation of different sulfides [a].

Entry	Substrate	Product	Conv. (%)	Sel. [b] (%)	TON	TOF（h^{-1}）
1	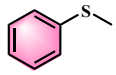	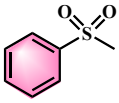	98.0	99.0	319.5	159.8
2	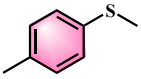	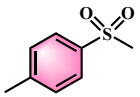	94.0	95.0	300.5	150.2
3		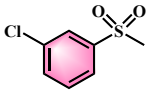	99.0	99.0	294.4	147.2
4	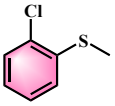	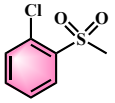	99.0	97.0	280.9	140.4
5	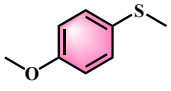	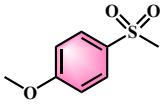	99.0	90.0	311.7	155.9
6	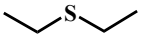	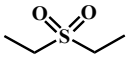	99.0	99.0	273.5	136.8
7	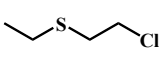	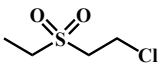	99.0	99.0	299.8	149.9
8	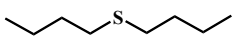	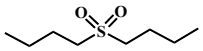	99.0	99.0	303.1	151.5

[a] Reaction conditions: 0.5 mmol MPS, 0.7 mmol % PW_{12}(32%)@TpTG material, 1.3 mmol H_2O_2, 25 °C 300 W xenon lamp and reaction time 2.0 h; [b] the main product of is sulfone.

$$\mathrm{TON} = \frac{n_{prod}}{n_{PW_{12}}} = \frac{n_{sub} C_{Conv.} C_{Sel.} M_{PW_{12}}}{m_{cat} w_{PW_{12}}}$$

$$\mathrm{TOF} = \frac{TON}{t}$$

References

[1] T. Huang, J. Kou, H. Yuan, H. Guo, K. Yuan, H. Li, F. Wang, Z. Dong, *Adv. Funct. Mater.*,

2025, **35**, 2413943.
[2] Q. Zhu, H. An, J. Fu, H. Sun, Y. Zhang, T. Q. Xu, *Inorg. Chem.*, 2025, **64**, 16223−16233.
[3] Q. Zhu, H. An, T. Q Xu, Y. Chen, Y. Wei, H. Sun, *ACS Sustain. Chem. Eng.*, 2024, **12**, 1655−1665.
[4] J. L. Chen, J. Y. Wang, X. Y. Liu, N. Xu, H. Li, X. L. Wang, *Inorg. Chem. Commun.*, 2026, **190**, 116937.
[5] C. Batalha, D. C. Fajardo, H. V. Filho, J. B. G. Bruziquesi, C. G. O. de Oliveira, L. C. A. Gonçalves, M. A. Ramalho, T. d. C. Silva, A. C. *Korean J. Chem. Eng.*, 2023, **40**, 2434−2441.